Molecular Biology of the Cell
Vol. 20, 1833–1844, March 15, 2009

RNA Interference Screen Identifies Usp18 as a Regulator of Epidermal Growth Factor Receptor Synthesis

Jason E. Duex and Alexander Sorkin

Department of Pharmacology, University of Colorado Denver, Aurora, CO 80045

Submitted August 27, 2008; Revised December 19, 2008; Accepted January 12, 2009
Monitoring Editor: Carl-Henrik Heldin

Elevated expression of epidermal growth factor receptor (EGFR) contributes to the progression of many types of cancer. Therefore, we developed a high-throughput screen to identify proteins that regulate the levels of EGFR in squamous cell carcinoma. Knocking down various ubiquitination-related genes with small interfering RNAs led to the identification of several novel genes involved in this process. One of these genes, Usp18, is a member of the ubiquitin-specific protease family. We found that knockdown of Usp18 in several cell lines reduced expression levels of EGFR by 50–80%, whereas the levels of other receptor tyrosine kinases remained unchanged. Overexpression of Usp18 elevated EGFR levels in a manner requiring the catalytic cysteine of Usp18. Analysis of metabolically radiolabeled cells showed that the rate of EGFR protein synthesis was reduced up to fourfold in the absence of Usp18. Interestingly, this dramatic reduction occurred despite no change in the levels of EGFR mRNA. This suggests that depletion of Usp18 inhibited EGFR mRNA translation. In fact, this inhibition required the presence of native 5′ and 3′ untranslated region sequences on EGFR mRNA. Together, our data provide evidence for the novel mechanism of EGFR regulation at the translational step of receptor synthesis.

INTRODUCTION

Epidermal growth factor (EGF) receptor (EGFR) is overexpressed in various human epithelial cancers, including breast, ovary, head and neck, renal, lung, and colorectal carcinoma (Rowinsky, 2004). These elevated levels of EGFR result in enhanced growth and survival signaling in cancer cells. Interestingly, in many types of cancer EGFR overexpression is not due to gene amplification (Grandis and Sok, 2004). In such cases, the mechanisms leading to high levels of EGFR are not well understood. To achieve a better understanding for cellular control of EGFR levels, much effort has been put into elucidating the mechanisms that control turnover of EGFR when cells are stimulated by ligand. These studies have shown that, under normal cellular receptor levels, cells have sufficient machinery to internalize activated receptors through the process of clathrin-mediated endocytosis (reviewed in Sorkin and Von Zastrow, 2002; Wiley, 2003). It seems that in many cancers, the high levels of EGFR overwhelm this machinery, leading to prolonged signaling and subsequent increases in cell proliferation and survival. Receptors that do become internalized are sorted for recycling back to the cell surface or onward to lysosomes where they are degraded, thus terminating signaling (receptor down-regulation). Trafficking of activated receptors to the lysosomal degradation pathway is promoted by ubiquitination of EGFR, with the E3 ubiquitin ligase Cbl playing a critical role in this process (Dikic and Giordano, 2003; Huang *et al*., 2006).

The extent of EGFR ubiquitination is determined by the competing activity of Cbl and deubiquitination enzymes (DUBs), providing yet another layer in the regulation of EGFR down-regulation (Komada, 2008). Receptor deubiquitination can reroute activated receptors from the degradation pathway, which results in their recycling back to the cell surface. In such a mechanism, inhibition of DUBs would abrogate this recycling mechanism and accelerate EGFR degradation. Such acceleration was observed with the inhibition of the endosomal DUB AMSH (McCullough *et al*., 2004; Bowers *et al*., 2006). Similarly, depletion of another DUB, Usp8 (UBPY), also led to changes in the degradation rate of EGFR and another receptor tyrosine kinase (RTK), c-Met (Mizuno *et al*., 2005; Bowers *et al*., 2006; Row *et al*., 2006; Alwan and van Leeuwen, 2007). However, the extent to which inhibition of these enzymes affected down-regulation of EGFR was rather partial, suggesting the existence of other DUBs that are effective in controlling the down-regulation of EGFR. With this idea in mind, we set out to identify additional DUBs that control EGFR turnover.

We used a library of small interfering RNAs (siRNAs) that target DUBs and other genes related to deubiquitination. These siRNAs were screened for their ability to alter cell surface levels of EGFR in a squamous cell carcinoma cell line. This screen revealed that depletion of the deubiquitination enzyme Usp18 (Ubp43) leads to a dramatic down-regulation in the steady-state levels of EGFR. Usp18 has an in vitro ability to remove ubiquitin from substrates (Liu *et al*., 1999; Schwer *et al*., 2000). However, the in vivo activity of Usp18 seems to be toward removing the ubiquitin-like molecule ISG15 from substrates (Malakhov *et al*., 2002, 2003). Our analysis uncovered a novel function of Usp18 in regulating EGFR synthesis at the mRNA translation step.

This article was published online ahead of print in *MBC in Press* (http://www.molbiolcell.org/cgi/doi/10.1091/mbc.E08–08–0880) on January 21, 2009.

Address correspondence to: Alexander Sorkin (alexander.sorkin@ucdenver.edu).

Abbreviations used: DUB, deubiquitination enzyme; EGFR, epidermal growth factor receptor; siRNA, small interfering RNA; UTR; untranslated region; YFP, yellow fluorescent protein.

MATERIALS AND METHODS

Antibodies

Monoclonal antibodies to EGFR (#528) were purified from hybridoma cells from American Type Culture Collection (Manassas, VA); antibodies to green fluorescent protein (GFP) and transferrin receptor were from Zymed Laboratories (San Francisco, CA); EGFR (#05-104) was from Millipore (Billerica, MA); α-actinin was from Millipore Bioscience Research Reagents (Temecula, CA) (MAB 1682); ErbB2 for SKBR3 and BT474 cells was from NeoMarkers (Fremont, CA); and ErbB2 for SCC2 cells was from Cell Signaling Technology (Danvers, MA) (29D8). Polyclonal antibodies to EGFR (#1005) and c-Met were obtained from Santa Cruz Biotechnology (Santa Cruz, CA).

Plasmid Constructs and siRNA

Usp18 cDNA was a generous gift from Dr. Dong Er Zhang (The Scripps Research Institute, La Jolla, CA). The cDNA was polymerase chain reaction (PCR) amplified using the forward ccgctcgagaccatgagcaaggcgtttgg and reverse cgcggatccgcactccatcttcatg primers, which added XhoI and BamHI restriction sites. The PCR was then cloned into XhoI–BamHI-gapped pEYFP-C3. Using the yellow fluorescent protein (YFP)-Usp18^{Wt} plasmid as a template, the YFP-Usp18^{C63S} construct was generated by site-directed mutagenesis, using the forward caacattggacagacctcctgccttaactccttg and reverse caaggagttaaggcaggaggtctgtccaatgttg primers. Generation of the EGFR-monomeric red fluorescent protein (mRFP) construct has been described previously (Galperin *et al*., 2004). Experiments performed with individual siRNA oligonucleotides used 21-nucleotide RNA duplexes obtained from Dharmacon RNA Technologies (Lafayette, CO) (nontargeting and Usp18#6) and QIAGEN (Valencia, CA) (Usp18#5). The sequences were as follows: siGENOME NonTargeting siRNA #2; Usp18#6 target sequence ccagggagUUaUcaagcaa; and Usp18#5 target sequence gggaagacauccagUgUac.

Cell Culture and Transfections

UMSCC2 head-and-neck squamous cell carcinoma (SCC) cells (further referred to as SCC2) were provided by Drs. Scott Weed and Barbara Frederick (UCD, Aurora, CO) and originated from Dr. T. Carey (University of Michigan, Ann Arbor, MI). The cells were grown in DMEM (Invitrogen, Carlsbad, CA) supplemented with 5% fetal bovine serum (FBS) (HyClone Laboratories, Logan, UT). African green monkey COS1, human breast carcinoma BT474 and SK-BR3 cells were grown in DMEM supplemented with 10% FBS. HeLa cells stably expressing EGFR-GFP were generated by limited-dilution cloning and selection for the resistance to Geneticin (G418; Invitrogen).

DNA transfections were performed using the standard QIAGEN protocol and Effectene reagent. Plated cells were incubated with DNA/lipid suspension at 37°C for 48 h before analysis. siRNA transfections using individual oligonucleotides were performed as per Dharmacon protocol. Briefly, siRNA duplexes were mixed with 1× siRNA universal buffer (Dharmacon RNA Technologies) and DMEM, whereas Dharmafect2 reagent was mixed with DMEM. After 5-min incubation, solutions were mixed for 20 min at room temperature (RT) followed by addition to plated cells for a final siRNA concentration of 100 or 150 nM. Transfections were repeated 24 h later, and the cells were used for experiments 72 h after the initial transfection.

siRNA High-Throughput Screen for EGFR Levels

A siRNA library targeting deubiquitinating enzymes and other ubiquitin-related genes was custom ordered (Dharmacon RNA Technologies) and received in 96-well format. A pool of four siRNA oligonucleotides were preplated per well, allowing for a reverse transfection approach to gene knockdown. Immediately before the addition of cells, a suspension of rehydration solution and transfection lipid (Dharmafect 2) was added to each well for 30 min at RT. SCC2 cells were added and the plates incubated at 37°C in 5% CO_2 for 72 h. Plates were treated with 100 ng/ml EGF (Thermo Fisher Scientific, Waltham, MA) and incubated at 37°C for 4 h. The cells were then washed with Ca^{2+}, Mg^{2+}-free phosphate-buffered saline (PBS) and fixed with freshly prepared 4% paraformaldehyde (Electron Microscopy Sciences, Hatfield, PA) for 12 min at RT. All immunolabeling steps were carried out in the absence of detergent to determine EGFR levels exclusively at the cell surface. The cells were first blocked with 0.5% bovine serum albumin (BSA)/PBS for 1 h before treatment with EGFR antibody #528 followed by secondary goat anti-mouse antibodies conjugated with horseradish peroxidase (HRP) (Jackson ImmunoResearch Laboratories, West Grove, PA). Amplex Red hydrogen peroxidase assay solution (Invitrogen) was added for 30 min at RT. The extent of HRP activity in each well, and therefore EGFR levels, was determined by analyzing the plates on an HTS7000 reader (excitation 530/emission 595; PerkinElmer Life and Analytical Sciences, Boston, MA). The plates were then washed and CyQUANT solution (Invitrogen) was added to determine the relative amount of DNA (corresponding to number of cells) in each well. After a 5-min incubation at RT, the plates were read on an HTS7000 reader (excitation 485/emission 535). EGFR surface levels (Amplex Red signal) were normalized to the cell number (CyQUANT signal) for each well. EGFR surface levels in cells treated with nontargeting siRNA and stimulated with EGF are shown as "zero" percent. EGFR surface levels of targeting siRNA treated cells are displayed as the percent decrease (lower surface EGFR levels) or increase (higher surface EGFR levels) from control nontargeting siRNA-treated cells.

Quantitative Real-Time PCR

Cells treated with siRNA for 72 h were washed and total RNA was isolated from confluent 60-mm dishes as per QIAGEN RNeasy Mini protocol. Samples were submitted to the University of Colorado Denver PCR Core for analysis using Applied Biosystems (Foster City, CA) ABI PRISM 7700 sequence detection system and TaqMan gene expression assays (EGFR: Hs00193306_m1; Usp18: Hs00276441_m1). mRNA data were normalized to rRNA.

Immunofluorescence Microscopy

EGFR immunofluorescence staining was carried out on SCC2 and COS1 cells 72 h posttransfection with siRNA and 48 h posttransfection with YFP-Usp18 constructs. Cells transferred to coverslips after 48 h were rinsed with PBS and fixed at RT with 4% paraformaldehyde in PBS for 15 min. Coverslips were washed with PBS followed by a 15-min treatment with 0.05% saponin/PEM buffer [80 mM K-piperazine-*N*,*N*′-bis(2-ethanesulfonic acid), pH 6.8, 5 mM EGFTA, and 1 mM $MgCl_2$). Coverslips were washed with PBS before treatment with NH_4Cl/PBS for 15 min. Subsequently, cells were probed with the EGFR antibody #528 in 0.05% saponin/0.1% BSA/PBS, washed with PBS, and then probed with secondary donkey anti-mouse conjugated to Cy3 in 0.05% saponin/0.1% BSA/PBS. Washed coverslips were mounted in Mowiol (Invitrogen). Coverslips were viewed using a Mariannas imaging workstation equipped with an Axiovert 200M inverted microscope (Carl Zeiss, Thornwood, NY), a Xenon light source, automated x-y-z controlled stage, and CoolSNAPHQ camera (Intelligent Imaging Innovations, Denver, CO). Images (z-stacks of 20 optical sections) were acquired at binning 2 × 2 mode. The total cellular EGFR signal was quantified by generating selection masks for background-subtracted images of each individual cell and calculating the sum of fluorescence intensity using the mask statistics module of the SlideBook 4.2 software. In YFP-Usp18 overexpression experiments, the sum of Cy3 fluorescence intensity (EGFR) was calculated for both YFP-expressing and nonexpressing cells. A mean value of the EGFR immunofluorescence signal from nonexpressing cells was determined for each slide. The total Cy3 fluorescence intensity in each YFP-expressing cell was then divided to the mean Cy3 fluorescence intensity of nonexpressing cells. The resulting ratios were then averaged for each experimental condition. The data were analyzed for statistical significance and plotted using GraphPad Prism 4 (GraphPad Software, San Diego, CA).

Live-Cell Microscopy

COS1 cells grown on glass coverslips were either transfected with siRNAs or DNA constructs (YFP-Usp18 and EGFR-mRFP) and used for experiments, respectively, 72 or 30 h later. The cells were incubated with 40 ng/ml EGF-Rh (Invitrogen) at 4°C for 45 min, rinsed with PBS, and further incubated in fresh media at 37°C for 30 min. The coverslips were mounted in the live-cell microscope chamber, and images were acquired using Cy3 (rhodamine and mRFP) and fluorescein isothiocyanate (YFP) filter channels at RT.

^{125}I-EGF Binding

These experiments were performed as reported previously (Huang *et al*., 2003). Briefly, SCC2 cells were treated with siRNA for 72 h before being placed on ice. ^{125}I-EGF was prepared as described previously (Huang *et al*., 2004) and added (20 ng/ml) to cells for 1 h at 4°C followed by washing with medium. Bound ^{125}I-EGF was then removed with acetic buffer, pH 2.8, and quantified on a gamma counter. The cell monolayer was washed with PBS to neutralize pH followed by total protein determination. Thus, the amount of ^{125}I-EGF was normalized to the amount of total cellular protein for each condition.

Extracts and Western Blot Analysis

Total cell lysates were prepared by lysing cells in TGH buffer (1% Triton X-100, 10% glycerol, and 50 mM HEPES, pH 7.3) supplemented with 150 mM NaCl, 2 mM EGTA, 2 mM EDTA, 1 mM phenylmethanesulphonylfluoride, and protease inhibitor cocktail. Sodium orthovanadate (1 mM) was included in the lysis buffer used in the experiments presented in Figure 2B but omitted in other experiments. Lysates were cleared with 14,000 × *g* centrifugation for 10 min, and supernatants were subjected to SDS-polyacrylamide gel electrophoresis (PAGE) followed by their transfer to nitrocellulose. Blots were subsequently blocked in 5% milk before probing with primary and secondary antibodies, followed by enhanced chemiluminescence-based detection (GE Healthcare, Piscataway, NJ) using x-ray films (Pierce Chemical, Rockford, IL).

[^{35}S]Methionine/cysteine Labeling

Cells were treated with siRNA for 72 h. To measure EGFR synthesis, fresh media were added consisting of DMEM lacking L-methionine and L-cysteine (Invitrogen) and 5% dialyzed FBS (HyClone Laboratories). The media were

supplemented with 300 μCi of protein labeling mix [^{35}S] (PerkinElmer Life and Analytical Sciences) per 60-mm dish and incubated at 37°C for the indicated time. To measure EGFR degradation, cells were incubated with ^{35}S-media for 4 h (300 μCi/60-mm dish) followed by washing in DMEM and recovery in complete DMEM supplemented with 5% FBS for 30 min. The cells were then chase incubated in the same medium for indicated times. In both types of experiments, the cells were washed at the end of the incubation or chase time with PBS followed by lysis in TGH buffer. Extracts were cleared by spinning at 14,000 $\times$ *g* for 10 min. mAb528 antibody was added to extracts and incubated at 4°C for 2 h to immunoprecipitate EGFR. Protein A-Sepharose beads (Zymed Laboratories) were added for an additional 1 h followed by pelleting at 1000 $\times$ *g*. Pellets were washed 1$\times$ in TGH supplemented with 500 mM NaCl, 1$\times$ with TGH supplemented with 150 mM NaCl, and 1$\times$ with TGH before subjecting samples to SDS-PAGE. Gels were dried onto filter paper and subjected to autoradiography and analyzed by Typhoon8600 Imager (GE Healthcare).

RESULTS

RNA Interference (RNAi) Screen Identifies Usp18 as a Potential Regulator of EGFR Levels

To identify proteins that promote EGFR down-regulation in cancer cells, we developed a high throughput screen that measures EGFR surface levels in the reverse transfection 96-well plate format (Boese *et al*., 2006; Sorkina *et al*., 2006). In this screen, we used head-and-neck SCC2 cells that express high levels of EGFR and require EGFR for growth (Frederick *et al*., 2007). The cells were grown in 96-well plates preloaded with siRNA pools (4 oligonucleotides). After 3 d, the amount of EGFR on the cell surface was measured by binding of the EGFR antibody #528 to formaldehyde-fixed cells followed by a quantitative immunochemical reaction. In proof of principle experiments, SCC2 cells were reverse-transfected in 96-well plates with nontargeting (control) siRNA or siRNA targeting genes whose knockdown has been shown previously to influence EGFR endocytosis (Huang *et al*., 2004). We observed that SCC2 cells incubated with siRNA pools targeting clathrin heavy chain or Grb2, when stimulated with EGF, displayed higher levels (46–57%) of surface EGFR when compared with nontargeting siRNA pools (Figure 1A). Conversely, SCC2 cells incubated with a siRNA pool targeting the deubiquitinase enzyme AMSH had a reduced amount (−37%) of surface EGFR, consistent with previous studies (McCullough *et al*., 2004; Bowers *et al*., 2006). These control experiments demonstrate the feasibility and accuracy of this screen.

We next applied this screen to a siRNA oligonucleotide library consisting of siRNA SmartPOOLs that target 106 different genes related to deubiquitination. Screening this library revealed several genes whose knockdown results in enhanced down-regulation of EGF-activated EGFR in SCC2 cells. The most prominent down-regulation of EGFR was observed in cells incubated with an Usp18 siRNA pool, which caused an EGF-induced 80% reduction in EGFR surface levels compared with control siRNA (Figure 1B).

Using the same EGFR reverse transfection siRNA 96-well format, each of the four siRNA duplexes from the Usp18 siRNA SmartPOOL were individually tested for their ability to down-regulate EGFR. We observed that three of four siRNAs augmented EGF-induced EGFR down-regulation to a similar extent as the SmartPOOL (Figure 1C). Therefore, these data demonstrate that the observed effect of Usp18 siRNA is specific and not due to off-target effects of these duplexes. For future experiments, we have chosen to use duplexes #5 and #6 because they demonstrated the greatest ability in our screen to promote EGFR down-regulation.

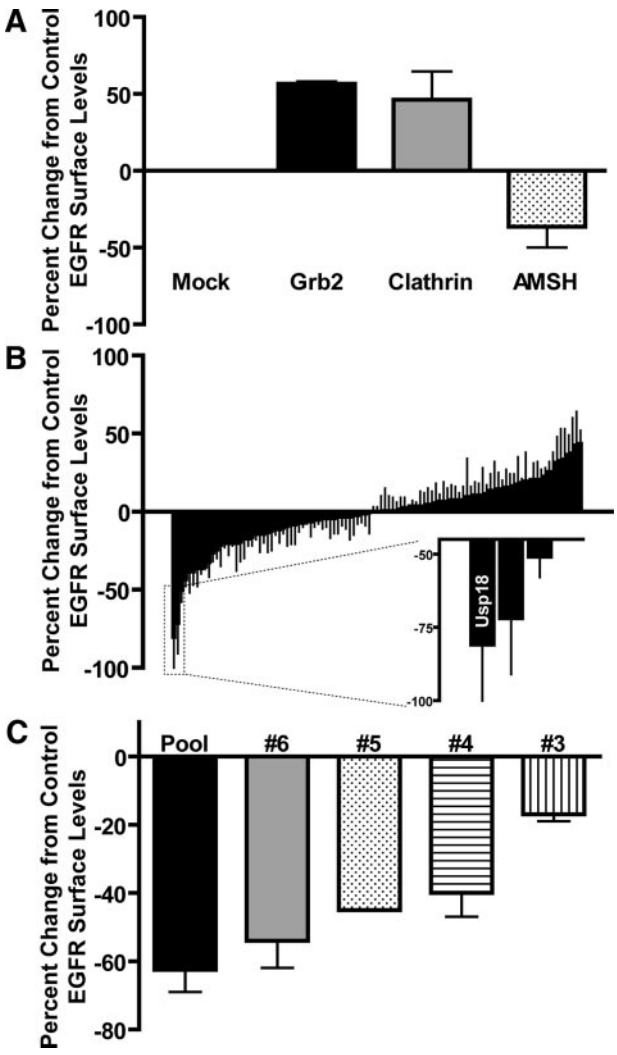

Figure 1. High-throughput screen identifies Usp18 as a potential regulator of EGFR down-regulation in cancer cells. (A) Changes in EGFR levels after knockdown of specific genes are consistent with previous studies. SCC2 cells were subjected to reverse siRNA transfection at a siRNA concentration of 75 nM. After 72 h, cells were treated with 100 ng/ml EGF for 4 h, and the surface levels of EGFR were quantitated using an enzyme-linked immunosorbent assay-like assay (see *Materials and Methods*). For normalization, zero represents the EGF-induced levels of surface EGFR found on control cells (those subjected to nontargeting siRNA). In cells that were subjected to targeting siRNA, the EGF-induced cell surface concentration of EGFR is displayed as the percentage of decrease (lower surface EGFR levels) or increase (higher surface EGFR levels) from control cells. (B) A siRNA library targeting 106 genes related to deubiquitination was screened and the surface levels of EGFR determined as described in *Materials and Methods*. An inset shows that a siRNA pool targeting Usp18 caused the most dramatic decrease in the surface levels of EGFR. (C) The individual siRNA oligonucleotides from the Usp18 SmartPOOL promote down-regulation of cell surface EGFR. SCC2 cells were reverse transfected with the Usp18 siRNA pool or each individual siRNA oligonucleotide. Surface levels of EGFR are displayed as in A. Data averaged from two different experiments. The values in all bar graphs of this study are averaged from three independent experiments unless otherwise noted. The error bars represent the SE of the mean.

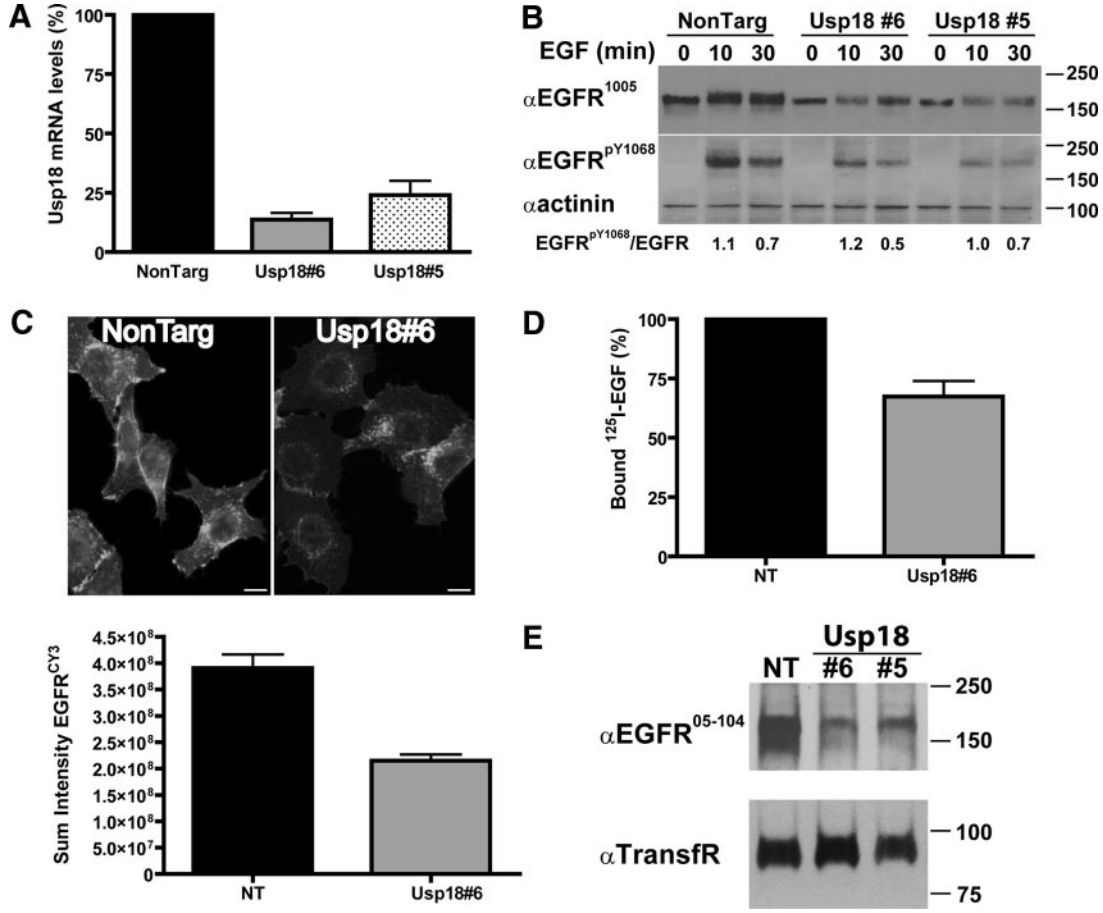

Figure 2. Multiple Usp18 siRNA oligonucleotides each dramatically reduce Usp18 expression and subsequently promote total cellular down-regulation of EGFR. (A) Usp18 mRNA levels are reduced up to 90% in SCC2 cells after Usp18 siRNA treatment. Nontargeting and Usp18 targeting siRNA oligonucleotides were forward transfected into SCC2 cells twice at 24-h intervals at a concentration of 150 nM. After 72 h, total RNA was isolated from these cells and Usp18 mRNA levels were determined by real-time PCR. The values for each sample were normalized to rRNA and then to nontargeting siRNA values. (B) Depletion of Usp18 from SCC2 cells leads to a 55% reduction in EGFR activation and total cellular EGFR levels. SCC2 cells were transfected with the indicated siRNA oligonucleotides (100 nM). After 72 h, cells were treated with 40 ng/ml EGF for the indicated times. Whole-cell lysates were subjected to Western blot analysis using $EGFR^{1005}$ (total EGFR), $EGFR^{pY1068}$ (phosphorylated EGFR), and α-actinin (loading control) antibodies. All Western blots in this study are representative of three or more experiments. The ratio of activated EGFR to total cellular EGFR was calculated and displayed below the blots. (C) EGFR immunofluorescence reveals that despite lower levels, EGFR cellular distribution does not significantly change after depletion of Usp18. SCC2 cells treated with siRNA were fixed, permeabilized with saponin, and subjected to immunofluorescence with $EGFR^{528}$ antibody. All fluorescence intensity settings are identical for the two images. Images were acquired in 20-stack z-series, and the total cellular EGFR signal was quantitated for each cell. Cells treated with Usp18 siRNA had an average 45% decrease in EGFR signal compared with control cells (bar graph). Data were obtained from a minimum of 12 cells. Bars, 10 μm. (D) SCC2 cells depleted of Usp18 have a reduced number of EGF binding sites on the cell surface. After transfection with siRNA, SCC2 cells were placed on ice and incubated with ^{125}I-EGF for 1 h. The amount of surface-bound ^{125}I-EGF is expressed as a percentage relative to control cells set to 100%. (E) Depletion of Usp18 from SCC2 cells leads to a 55% reduction in total cellular EGFR levels. SCC2 cells were transfected with the indicated siRNA as in B. Whole-cell lysates were subjected to Western blot analysis by using antibody $EGFR^{05\text{-}104}$ (recognizing the extracellular domain of EGFR) and an antibody to the transferrin receptor (TransfR).

Usp18 siRNA Efficiently Targets Usp18 and Leads to a Dramatic Decrease in Steady-State EGFR Protein Levels

Testing the efficiency and specificity of the individual Usp18 siRNA duplexes in knocking down Usp18 protein was necessary to confirm the results of the screen. All commercially available antibodies to Usp18 were tested, but none were able to obtain specific detection of Usp18 in human cells. Therefore, we examined Usp18 siRNA effectiveness using real-time PCR. In addition, all subsequent siRNA experiments were performed using forward transfection, the more conventional approach in which siRNA duplexes are added to cells. Such analysis revealed that Usp18 mRNA levels were reduced up to 90% after treatment with Usp18#6 or Usp18#5 siRNAs (Figure 2A). Thus, two different Usp18 siRNA duplexes, when added to SCC2 cells, demonstrated a near complete knockdown of Usp18 expression.

To determine whether Usp18 depletion can affect the total cellular levels of EGFR, whole-cell lysates from cells treated with Usp18 siRNAs were probed for EGFR by Western blotting. As shown in Figure 2B and Supplemental Figure 1A, a 55 or 50% decrease in total EGFR levels was induced by either Usp18#6 or Usp18#5 duplexes, respectively. The amount of activated EGFR measured by the extent of phosphorylation of Tyr1068 was correspondingly reduced in the absence of Usp18 (Figure 2B). Surprisingly, depletion of Usp18 led to a substantial decrease in EGFR levels even in

the absence of EGF (Figure 2). These experiments suggest that Usp18 controls total cellular levels of EGFR under the steady-state conditions of SCC2 cell growth.

To test whether knockdown of Usp18 alters the subcellular distribution of the receptor, the localization of EGFR immunoreactivity was analyzed by fluorescence microscopy. SCC2 cells were depleted of Usp18 followed by detergent permeabilization and immunofluorescence staining. In this and several subsequent experiments, we commonly used only Usp18#6 siRNA because this duplex had the maximal effect on both Usp18 and EGFR expression levels. Quantification of the EGFR immunofluorescence signal in individual cells revealed an ~45% decrease in receptor levels in Usp18#6-treated cells relative to nontargeting siRNA-treated cells (Figure 2C). This decrease in the total amount of EGFR measured in detergent-permeabilized cells was comparable with the decrease in the surface levels of EGFR measured in nonpermeabilized cells depleted of Usp18 by using the same EGFR antibody (Figure 1C). No obvious differences in the pattern of EGFR localization between control and Usp18-depleted cells were observed. It seems that there was less EGFR on the cell surface and in intracellular membranes in cells deprived of Usp18. Furthermore, a decrease in the plasma membrane concentration of EGFR was confirmed using a ^{125}I-EGF binding assay at 4°C (Figure 2D).

Finally, we investigated the possibility that posttranslational modifications in the cytosolic domain of EGFR could hinder EGFR antibody #1005 recognition, thus presenting a false decrease in EGFR by Western blot analysis. To this end, whole-cell lysates from SCC2 cells treated with control or Usp18 siRNA were analyzed by Western blotting using EGFR antibody #05-104 that recognizes an epitope on the extracellular domain of EGFR. This approach also showed that total cellular levels of EGFR were decreased by 50% upon depletion of Usp18 (Figure 2E). In contrast, treatment of SCC2 cells with Usp18 siRNA had no effect on the expression level of the transferrin receptor (Figure 2E).

Together, the data in Figure 2 show that treatment of SCC2 cells with two individual Usp18 siRNA duplexes leads to a similarly efficient depletion of Usp18 mRNA. Such treatment also leads to a dramatic reduction in the steady-state levels of both surface and total cellular pools of EGFR as demonstrated by multiple methodological approaches.

Depletion of Usp18 Does Not Affect the Levels of Other RTKs

To test whether Usp18 depletion regulates EGFR specifically or can also regulate other RTKs, we measured the effects of Usp18 depletion on the levels of ErbB2, another member of the EGFR/ErbB receptor tyrosine kinase family. In SCC2 cells treated with Usp18 siRNA, we observed a dramatic decrease in the levels of EGFR, but no change in the amount of ErbB2 protein (Figure 3). Moreover, the protein levels of another RTK, hepatocyte growth factor receptor (c-Met), were unchanged upon depletion of Usp18 in SCC2 cells. Treatment of the breast cancer cell lines SKBR3 or BT474 with Usp18 siRNA did not affect ErbB2 levels despite the strong reduction in EGFR levels in SCC2 cells in the same experiments (Figure 3). In agreement with our data, a previous study showed that the levels of interferon receptor, at the cell surface or throughout the cell, were not altered in Usp18−/− mouse embryonic fibroblasts (Malakhova *et al.*, 2006). These observations strongly suggest that Usp18 is regulating EGFR with a high level of specificity.

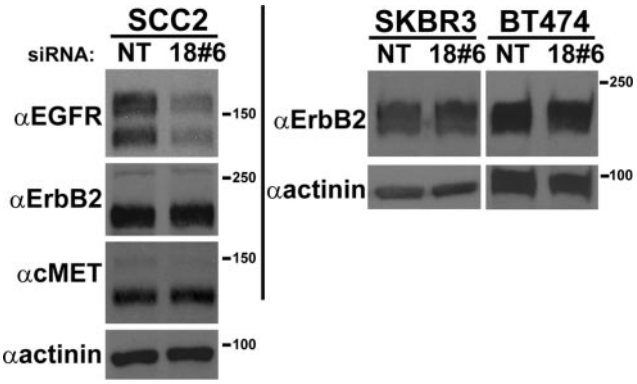

Figure 3. Depletion of Usp18 does not affect the protein levels of other receptor tyrosine kinases. SCC2 and indicated breast cancer cell lines were transfected with Usp18#6 siRNA and control siRNA (100 nM). Whole-cell lysates were then analyzed by immunoblotting for EGFR, ErbB2, and c-Met.

Depletion of Usp18 in COS1 Cells Also Leads to a Dramatic Decrease in EGFR Levels

Because SCC2 cells have the technical limitation of very poorly expressing ectopic DNA, we used COS1 (African green monkey) cells for additional experiments. Relative to SCC2, COS1 cells are readily transfectable with DNA plasmids, have lower levels of EGFR, and have a superior morphology for microscopy experiments. We first set out to determine whether human Usp18 siRNA was able to inhibit expression of COS1 Usp18 mRNA. Real-time PCR experiments confirmed that Usp18 is expressed in these primate cells and demonstrated that Usp18#6 siRNA leads to a 90% reduction in the expression of Usp18 mRNA in COS1 cells (Figure 4A).

The ability of COS1 cells to efficiently express DNA constructs allowed us to test the specificity of Usp18 siRNAs. We determined that both Usp18#6 and Usp18#5 siRNA completely blocked expression of YFP-tagged Usp18 (YFP-Usp18) while having no effect on expression of YFP alone (Figure 4B). Analysis of total cellular EGFR levels revealed that treatment of COS1 cells with either Usp18#6 or Usp18#5 siRNAs resulted in a dramatic decrease in the levels of receptor (Figure 4C). In fact, EGFR down-regulation in COS1 cells was 85%, a significant increase over the 55% decrease observed in SCC2 cells. Furthermore, as observed in SCC2 cells, the levels of transferrin receptor remained unchanged.

The dramatic effect of Usp18 siRNA on EGFR in SCC2 cells resulted in the significant impairment of radiolabeled EGF binding to Usp18-depleted cells. Similarly, Figure 4D demonstrates a substantially lower amount of EGF-rhodamine conjugate (EGF-Rh) in endosomes of COS1 cells treated with Usp18 siRNA and incubated with EGF-Rh for 30 min (Figure 4D). Together, the data presented in Figure 4 show that treatment of COS1 cells with Usp18 siRNA leads to almost complete knockdown of Usp18 expression and an even more dramatic down-regulation of EGFR than what was observed in SCC2 cells.

Usp18 Overexpression Leads to EGFR Up-Regulation

The observation that Usp18 depletion results in a decrease in the levels of EGFR leads to the hypothesis that overexpression of Usp18 results in an increase in the levels of EGFR. To test this hypothesis, the amount of EGFR in COS1 cells overexpressing Usp18 was examined using a single-cell immunofluorescence assay. Quantification of EGFR immuno-

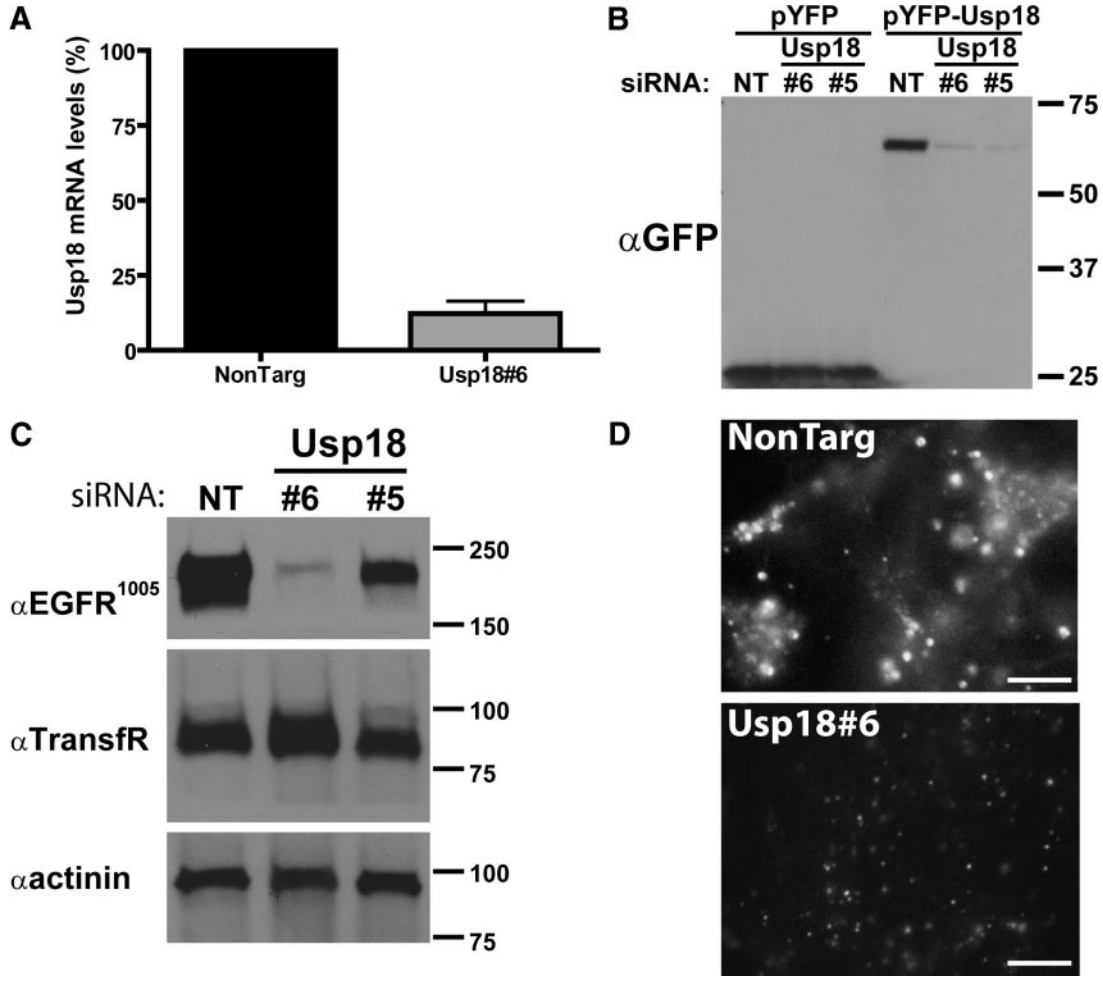

Figure 4. Usp18 depletion leads to EGFR down-regulation in COS1 monkey cells. (A) Usp18#6 siRNA treatment of COS1 cells leads to a 90% decrease in Usp18 mRNA. COS1 cells were transfected with siRNA (150 nM) and Usp18 mRNA levels measured by real-time PCR as in Figure 2A. (B) Usp18 siRNA blocks expression of ectopic Usp18. COS1 cells were transfected with the indicated siRNA (100 nM) for 24 h. The cells were then cotransfected with siRNA (30 nM) and pYFP-Usp18 or pYFP DNA plasmid (700 ng). Whole-cell lysates were analyzed by Western blot with GFP antibodies. (C) Total cellular EGFR levels are reduced by 85% in COS1 cells depleted of Usp18. The same COS1 cells used for Usp18 mRNA analysis were split and whole-cell lysates were subjected to Western blot analysis with $EGFR^{1005}$ antibody and antibodies to unrelated proteins. (D) Usp18 depletion significantly inhibits uptake of EGF-Rh. COS1 cells were transfected with siRNA as described in A and incubated with EGF-rhodamine for 45 min at 4°C before chasing without EGF-Rh for 30 min at 37°C. Images are representative of multiple acquisitions. All fluorescence intensity settings are identical for the two images. Bars, 10 μm.

fluorescence signals was carried out on three-dimensional images of individual cells. Such analysis revealed that overexpression of YFP-Usp18 significantly increased the EGFR expression level relative to both nonexpressing cells and control cells expressing YFP (Figure 5).

To test whether the isopeptidase activity of Usp18 is important for regulating EGFR expression levels, a $Usp18^{C63S}$ inactive mutant (corresponding to mouse $Usp18^{C61S}$; Malakhova *et al.*, 2006) was generated and expressed in COS1 cells. The expression level of this mutant was similar to that of wild-type YFP-Usp18. Interestingly, quantitative immunofluorescence analysis of cells overexpressing the inactive YFP-$Usp18^{C63S}$ mutant showed that this mutant did not increase cellular levels of EGFR compared with nonexpressing cells from the same slides (Figure 5).

These data support a model whereby increased levels of Usp18 lead to increased levels of EGFR and decreased levels of Usp18 lead to EGFR down-regulation. These data also suggest that the isopeptidase activity of Usp18 may be important for its ability to regulate EGFR expression levels.

YFP-tagged Usp18 Does Not Colocalize with EGFR

To begin elucidating the mechanisms by which Usp18 regulates EGFR levels, the localization of EGFR and YFP-tagged Usp18 was compared in COS1 cells. YFP-Usp18 showed a predominantly diffuse, cytosolic staining pattern with a small number of punctae (Figure 6A). A similar cytosolic localization was observed with GFP-Usp18 in HeLa cells (Schwer *et al.*, 2000). Analysis of COS1 cells overexpressing EGFR-mRFP along with YFP-Usp18 revealed no colocalization between the punctae of the two proteins regardless of whether the cells were treated with EGF (Figure 6A). When COS1 cells were incubated with EGF-Rh for 30 min at 37°C, no colocalization between YFP-Usp18 punctae and EGF-Rh containing endosomes was observed (Figure 6B). In fact, no colocalization was observed up to 70 min of continuous EGF-Rh internalization (data not shown). Furthermore, YFP-Usp18 punctae did not colocalize with endocytosed Texas Red-labeled transferrin nor Texas Red-labeled dextran (data not shown), confirming no endosome/lysosome-specific lo-

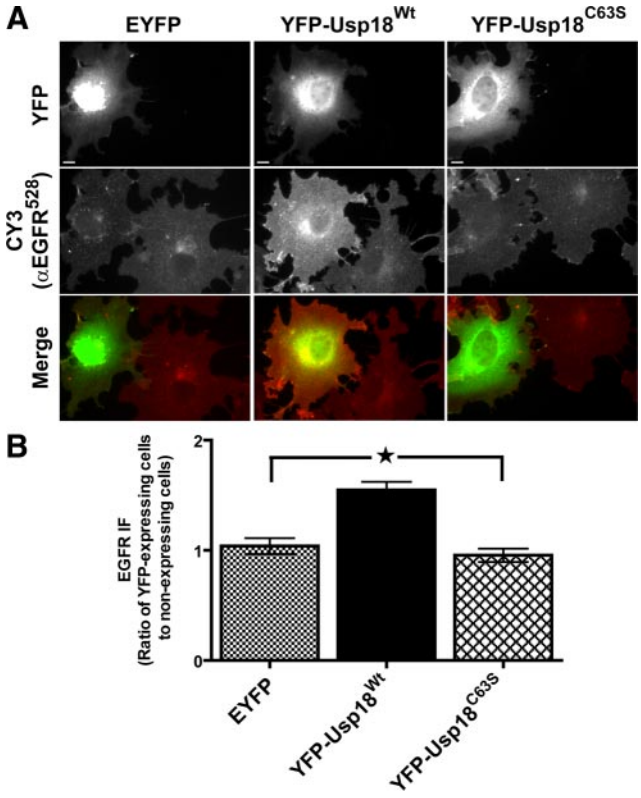

Figure 5. Overexpression of Usp18 leads to an up-regulation in total cellular levels of EGFR. (A) Representative images of COS1 cells overexpressing YFP, YFP-Usp18^{Wt}, or YFP-Usp18^{C63S}. The cells were transfected with the indicated DNAs and after 48 h, the cells were fixed, permeabilized with saponin, and subjected to immunofluorescence staining with αEGFR^{528} antibody. Images were acquired in 20-stack z-series. Individual optical sections are shown. Bars, 10 μm. (B) Quantification of the EGFR immunofluorescence signals in cells overexpressing YFP, YFP-Usp18^{Wt}, or YFP-Usp18^{C63S}. Elevated expression of Usp18^{Wt} leads to a 1.6-fold increase in the total cellular levels of EGFR whereas expression of YFP or YFP-Usp18^{C63S} did not affect EGFR levels. The total cellular EGFR immunofluorescence signal was measured in individual cells as described in *Materials and Methods*. Values are shown as the ratio of EGFR signal in YFP-expressing cells to EGFR signal in cells that do not express a YFP construct on the same coverslip. Data are averaged from three independent experiments and from 31 cells expressing YFP, 67 cells expressing YFP-Usp18^{Wt}, or 38 cells expressing YFP-Usp18^{C63S}. *$p < 0.001$.

calization of the YFP-Usp18 punctae. These data suggest that Usp18 does not colocalize with EGFR or compartments involved in EGFR endocytosis; therefore, Usp18 is unlikely to directly regulate trafficking of the EGFR protein.

EGFR Synthesis Is Dramatically Decreased Upon Depletion of Usp18

We have shown that when SCC2 or COS1 cells are depleted of Usp18, there is a corresponding dramatic decrease in total cellular levels of the EGFR protein. However, we also observed that the remaining EGFR maintains its normal cellular distribution. Such observations led to the hypothesis that cells lacking Usp18 have lower levels of EGFR due to changes in the rates of EGFR turnover. As a first step toward addressing this hypothesis, we determined the rate of EGFR synthesis in cells depleted of Usp18. SCC2 cells were treated with siRNA for 3 d, followed by incubation with [^{35}S]methionine/cysteine containing media. From these cells, EGFR was immunoprecipitated at various times to measure the rates of [^{35}S]methionine/cysteine incorporation. The rate of EGFR synthesis in SCC2 cells treated with Usp18 siRNA was ~50% the rate of control cells (Figure 7A). Such a result is consistent with the 50% reduction in EGFR levels observed in both Western blot (Supplemental Figure S1A and Figures 2B, 2E, and 3) and immunofluorescence analysis (Figure 2C) of SCC2 cells depleted of Usp18. In COS1 cells depleted of Usp18, the rate of EGFR synthesis was reduced by ~80% compared with control cells (Figure 7B). Such a dramatic effect in these cells is also in agreement with the Western blot analysis (Supplemental Figure S1B and Figure 4C). Together, these experiments show that depletion of Usp18 from SCC2 and COS1 cells leads to a dramatic reduction in the rate of EGFR synthesis. Furthermore, the extent of the reduction directly correlates with the reduction in whole-cell EGFR levels as determined by multiple analyses. Such observations strongly suggest that the decrease in EGFR protein levels after depletion of Usp18 is the direct result of a decrease in Usp18 synthesis.

EGFR Degradation Is Slightly Increased in the Absence of Usp18

To investigate whether depletion of Usp18 also alters EGFR degradation the rate of EGFR turnover was measured in cells treated with Usp18 siRNA. SCC2 cells were treated with siRNA for 3 d before being pulse-labeled with [^{35}S]methionine/cysteine containing media and then chased in complete, nonradioactive media. During this chase, EGFR was immunoprecipitated and analyzed over time for the disappearance of radiolabeled EGFR. This approach revealed that EGFR was degraded at a slightly faster rate in SCC2 cells treated with Usp18 siRNA compared with those cells treated with nontargeting siRNA (Figure 8A). The same analysis in COS1 cells also revealed a moderately increased rate of EGFR degradation in the absence of Usp18 (Figure 8B). However, this small increase in degradation rate cannot account for the significant increase in EGFR down-regulation observed in SCC2 and COS1 cells depleted of Usp18. Importantly, the amount of radiolabeled EGFR at time zero and total amount of cellular EGFR were substantially different between cells treated with Usp18 siRNA and control cells (Figure 8, A and B) due to different rates of biosynthesis (Figure 7, A and B). Therefore, it is likely that the increased rate of degradation is the result of lower levels of EGFR in these cells. In support of this, rates of EGFR degradation inversely correlate with the expression levels of EGFR, presumably due to saturation of cellular degradation machinery (Stoscheck and Carpenter, 1984a,b). In further support of this view, we found that inhibiting lysosomal activity by leupeptin or chloroquine treatment did not rescue the decrease in EGFR levels observed in the absence of Usp18 (Supplemental Figure S2).

EGFR mRNA Levels Are Unchanged Upon Depletion of Usp18

Based on the observation that EGFR biosynthesis is dramatically decreased upon depletion of Usp18, we investigated whether this decrease was the result of inhibition of EGFR gene expression in the absence of Ups18. Analysis of EGFR mRNA levels using real-time PCR demonstrated that EGFR mRNA levels in SCC2 cells were not statistically different between control and Usp18 siRNA-transfected cells (Figure 9A). Essentially similar results were obtained in COS1 cells (Figure 9B). Although a trend to slightly reduced levels of EGFR mRNA was observed in cells treated with duplex #6,

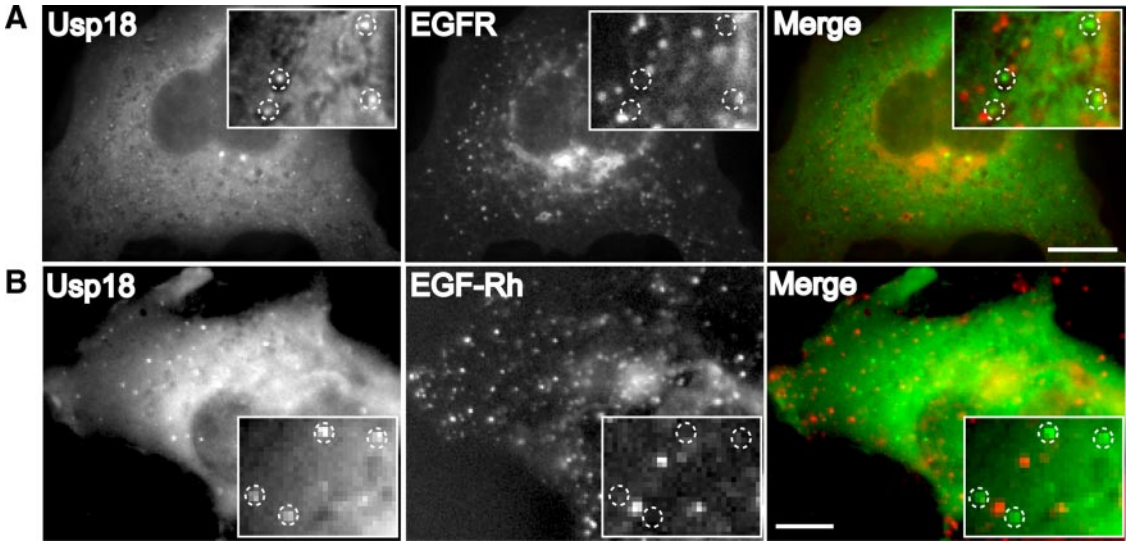

Figure 6. Absence of colocalization of YFP-Usp18 and EGFR. (A) Ectopic EGFR-mRFP does not colocalize with Usp18 punctae. COS1 cells were cotransfected with EGFR-mRFP and YFP-Usp18. Cells were later treated with 40 ng/ml EGF for 30 min followed by live-cell imaging. (B) Usp18 punctae do not colocalize with internalized EGFR ligand. COS1 cells transfected with YFP-Usp18 were incubated with 40 ng/ml EGF-Rh at 4°C, followed by a 30-min chase at 37°C and live-cell imaging.

such a small reduction in mRNA levels could not account for the dramatic changes in EGFR biosynthesis in cells transfected with this siRNA duplex (Figure 7). Therefore, Usp18 does not regulate EGFR mRNA production or turnover but more likely controls EGFR protein levels by regulating EGFR mRNA translation.

Usp18 Is Unable to Regulate EGFR mRNA When Native UTR Sequences Are Absent

Cells control mRNA translation principally through the 5′ and 3′ untranslated regions (UTRs) of mRNA molecules. To test the hypothesis that Usp18 regulates EGFR translation through the UTR sequences of EGFR mRNA, expression levels of EGFR and EGFR-GFP (lacking native EGFR 5′ and 3′ UTR sequences) were compared in cells depleted of Usp18. To this end, a HeLa cell line that stably expresses EGFR-GFP was generated. Usp18 depletion in these cells resulted in a dramatic decrease in the levels of endogenous EGFR (Figure 9C), similar to the decrease observed in COS1 cells (Figure 4C). In contrast, expression levels of EGFR-GFP were not affected by treatment with Usp18 siRNA duplexes #6 and #5 (Figure 9, C and D). Consistent with this result, we also observed that Usp18 depletion did not affect untagged, ectopic EGFR (lacking native UTRs) stably expressed in squamous cell carcinoma cells (data not shown). These observations show that EGFR genes lacking endogenous 5′ and 3′ UTR sequences are resistant to Usp18 regulation. Therefore, our data strongly suggest that Usp18 controls EGFR biosynthesis by regulating translation from EGFR mRNA and that the UTR sequences of EGFR mRNA are the site of Usp18 regulation.

DISCUSSION

In an attempt to identify previously unknown regulators of EGFR protein levels, a novel screen was developed that incorporated an siRNA library targeting the genes of DUBs and related proteins. This screen is based on whole-cell population measurements of EGFR expression rather than on single-cell analysis previously used in a RNAi library screening analysis of EGF endocytosis (Pelkmans *et al.*, 2005). The critical feature of our screening approach was the incorporation of a second parameter, total cellular DNA. Such an approach resulted in a normalized EGFR signal which provided a highly reliable comparative analysis between individual wells of the 96-well plate. Such normalization is critical in this type of screening analysis because cellular exposure to inhibitors such as siRNA can lead to toxicity and different growth rates due to on- and off-target effects.

Our analysis revealed that knockdown of Usp18 results in the dramatic down-regulation of EGFR. This phenotype was observed with three different Usp18 siRNA oligonucleotides and in three different cell lines from two different species. Interestingly, our data show that, unlike other DUBs such as AMSH and Usp8, Usp18 does not control EGFR down-regulation by regulating trafficking of ligand-activated internalized EGFR. Instead, Usp18 controls constitutive EGFR protein synthesis by regulating translation from EGFR mRNA. As an indication of the importance of Usp18 in EGFR synthesis, depletion of Usp18 results in a dramatic decrease (50–85%) in steady-state levels of EGFR protein.

Another surprising aspect of Usp18 function is its high specificity toward EGFR regulation. A previous study showed that Usp18−/− mouse cells had the same levels of interferon receptor as wild-type cells (Malakhova *et al.*, 2006). Consistent with this, our analysis revealed that protein levels of several other receptors were unaffected by Usp18 knockdown in human cells. For example, the absence of Usp18 had no effect on the steady state levels of the constitutively recycled transferrin receptor. Even more interesting was the observation that the levels of another ErbB family member, as well as another receptor tyrosine kinase (c-Met), were unaffected by Usp18 depletion. In contrast, other DUBs, such as AMSH and Usp8, regulate endosomal sorting of both EGFR and c-Met (Row *et al.*, 2006).

The observation that Usp18 depletion leads to a dramatic reduction in EGFR protein synthesis, despite normal EGFR mRNA levels, suggests Usp18 regulates EGFR mRNA in a manner not involving regulation of mRNA turnover. It is

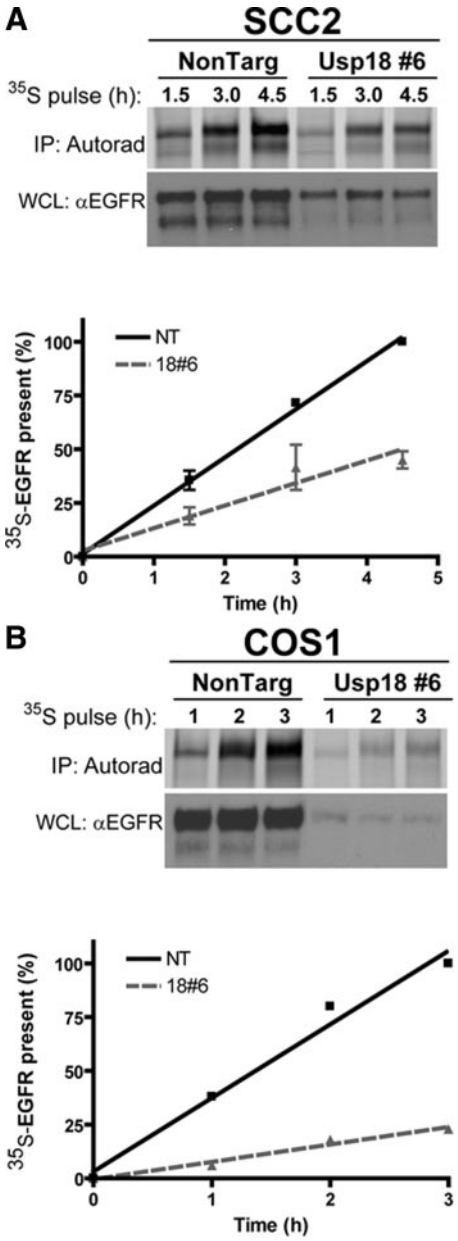

Figure 7. The rate of EGFR synthesis is dramatically decreased after depletion of Usp18. (A) EGFR synthesis rate is dramatically reduced in SCC2 cells treated with Usp18#6 siRNA. After siRNA transfection, [^{35}S]methionine-containing media were added to SCC2 cells. EGFR was subsequently immunoprecipitated at the indicated times, and ^{35}S incorporation into EGFR was measured through autoradiography. The 4.5 h (SCC2) or 3 h (COS1) nontargeting siRNA samples were set as 100%. Western blot analysis of the same labeled whole-cell lysates confirmed EGFR down-regulation after Usp18 depletion. The data are averaged from two experiments. (B) The rate of EGFR synthesis is reduced even more dramatically in COS1 cells treated with Usp18#6 siRNA. The data were obtained and are presented as described in A.

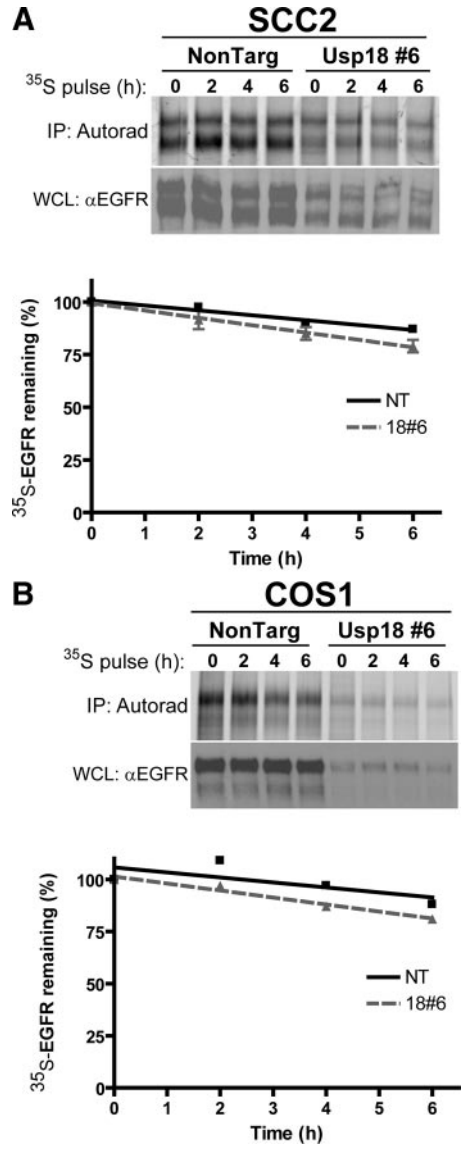

Figure 8. The EGFR degradation rate is slightly increased after depletion of Usp18. (A and B) SCC2 and COS1 cells, respectively, display a small change in the rate of EGFR degradation after depletion of Usp18. After transfection with siRNA, the cells were incubated in [^{35}S]methionine containing media for 4 h at 37°C, followed by a chase incubation in complete media for the indicated times. EGFR was immunoprecipitated and the amount of ^{35}S-labeled EGFR was measured by autoradiography. The data are expressed as 100% ^{35}S-EGFR remaining at time zero. Western blot analysis of the same labeled whole-cell lysates confirmed EGFR down-regulation after Usp18 depletion.

highly unlikely that Usp18 regulates EGFR mRNA by controlling EGFR pre-mRNA processing, a process that occurs in the nucleus. First, the real-time PCR analysis used to measure EGFR mRNA levels used a probe spanning an exon–exon boundary. The fact that EGFR mRNA levels were the same in the presence and absence of Usp18 suggests that under both conditions the EGFR transcript is spliced normally. Second, YFP-Usp18 shows no nuclear localization (Figure 6; Schwer *et al.*, 2000) and therefore most likely regulates only mature mRNA. Third, depletion of Usp18 had no effect on the expression levels of an ectopic EGFR-GFP construct. This construct differed from endogenous EGFR transcripts in that it lacked both EGFR introns and native EGFR UTR sequences. Together, these observations strongly suggest that Usp18 controls cytoplasmic protein translation from EGFR mRNA via the 5′ or 3′ UTR sequences.

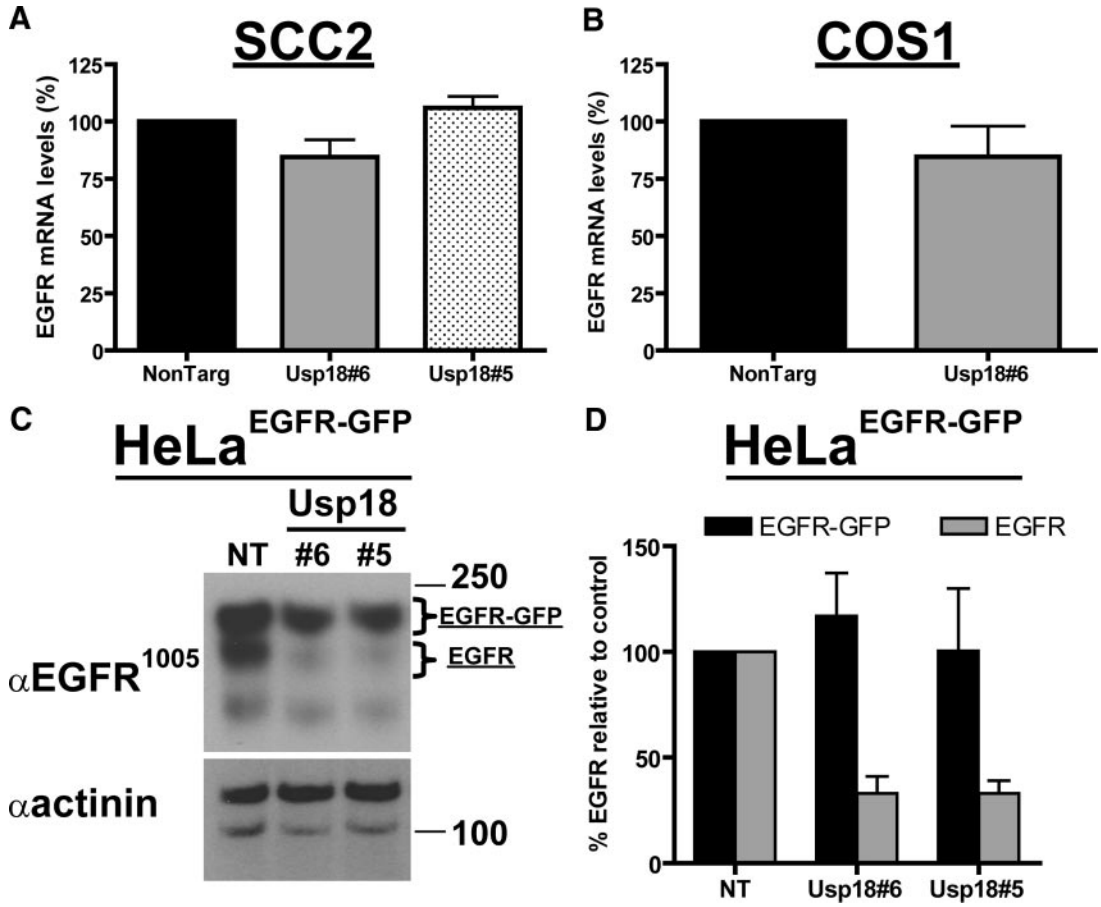

Figure 9. Effect Usp18 depletion has on EGFR levels requires endogenous EGFR mRNA. (A and B) EGFR mRNA levels are not affected by depletion of Usp18. SCC2 and COS1 cells, respectively, were transfected with siRNA (150 nM), and the levels of EGFR mRNA were determined using real-time PCR. (C) Usp18 depletion dramatically inhibits translation from native EGFR mRNA but not from EGFR mRNA lacking native UTR sequences. HeLa cells stably expressing EGFR-GFP were treated with Usp18 siRNA and the protein levels of endogenous EGFR and EGFR-GFP were determined using Western blot analysis. (D) EGFR and EGFR-GFP protein levels were quantitated from C and two additional similar experiments with HeLa/EGFR-GFP cells.

The precise manner by which Usp18 operates to regulate EGFR mRNA translation remains to be determined. Clearly, general machineries that handle mRNA processing are unlikely regulated by Usp18 because the effect of Usp18 depletion is highly specific to EGFR mRNA. One potential mechanism is that, in the absence of Usp18, EGFR mRNA translation is inhibited by the up-regulation of one or more microRNAs (miRNAs). Two recent reports have shown that specific miRNAs may regulate EGFR protein levels. Expression of miRNA-7 was shown to be down-regulated in glioblastomas, which normally have high levels of EGFR protein (Kefas *et al*., 2008). Furthermore, transfection of these cells with pre-miRNA-7 reduced EGFR mRNA translation. Another report demonstrated that treatment of a lung cancer cell line with an inhibitor to miRNA-128b led to an increase in EGFR protein levels without affecting the levels of EGFR mRNA (Weiss *et al*., 2008). Such an observation suggests that miRNA-128b can repress EGFR mRNA and it does so without accelerating mRNA decay. These data are strikingly similar to our results that imply that Usp18 knockdown leads to EGFR mRNA repression without promoting mRNA degradation.

mRNA repression can also occur independently from changes in mRNA levels by its sequestration into cytoplasmic processing bodies (PBs) and/or stress granules (SGs) (reviewed in Parker and Sheth, 2007). This mechanism has been implicated in the regulation of tumor necrosis factor-α protein expression (Kedersha *et al*., 1999; Piecyk *et al*., 2000). Analysis of the localization of YFP-Usp18 punctae in COS1 cells relative to markers of PBs and SGs (Hedls, TIA-1, and HuR), however, did not reveal any colocalization (data not shown). It should be emphasized that mRNA sequestration and miRNA inhibition are not mutually exclusive. Recent studies have demonstrated that PBs and SGs also contain proteins associated with miRNA function (Jakymiw *et al*., 2005; Liu *et al*., 2005a,b; Pillai *et al*., 2005). Analysis of changes in miRNA levels after depletion of Usp18 is in progress in our laboratory.

The hypothesis of RNA sequestration in PBs or SGs after depletion of Usp18 is also consistent with data showing Usp18−/− mice being resistant to viral infection (Malakhova *et al*., 2003; Ritchie and Zhang, 2004; Knobeloch *et al*., 2005). The decrease in viral replication in the absence of Usp18 could be due to sequestration of viral RNA into PBs and SGs, a process that, in this model, would be blocked by Usp18 after interferon stimulation (reviewed in Beckham and Parker, 2008). Congruently, under steady-state conditions, incorporation of EGFR mRNA into PBs or SGs could be blocked by Usp18.

Yet another possible mechanism by which Usp18 may regulate EGFR mRNA translation is by controlling ISG15 modification of an unknown EGFR mRNA translational regulator. This possibility is supported by our observation that in contrast to overexpression of wild-type Usp18, overexpression of isopeptidase inactive Usp18^{C63S} mutant did not result in increased EGFR levels (Figure 5). Additional support for this possible mechanism comes from the recent finding of ISG15 conjugation to human P56 (Zhao *et al*., 2005). P56 strongly interacts with the translation initiation factor 3 and has been shown to inhibit protein synthesis both in vitro and in vivo (Guo *et al*., 2000). Thus, future studies should investigate the potential role of ISG15-modified proteins such as P56 in the regulation of EGFR mRNA translation.

The fact that Usp18 depletion leads to a dramatic down-regulation in steady-state levels of EGFR protein suggests that inhibition of Usp18 has potential as a new strategy for EGFR-directed therapy. Such a strategy could be advantageous over or complementary to those strategies that currently target proteins regulating ligand-activated EGFR. First, down-regulation of steady-state EGFR levels could be a useful strategy in minimizing transforming signals induced by dimerization of EGFR (ErbB1) with ErbB2. Current approaches involving inhibition of EGFR kinase activity do not prevent tyrosine phosphorylation of EGFR by ErbB2 and thus do not prevent signaling through this pathway. Second, regulating the steady-state levels of EGFR could be a new approach to inhibiting the activity of the constitutively active, oncogenic EGFR variant III mutant, which lacks the ligand binding domain (Yamazaki *et al*., 1990; Nishikawa *et al*., 1994; Batra *et al*., 1995; Nagane *et al*., 1996). In summary, a further understanding of the mechanisms by which Usp18 controls EGFR should allow for a better evaluation of the potential this protein holds in being a new therapeutic target in EGFR-dependent tumors.

ACKNOWLEDGMENTS

We thank Dr. Dong Er Zhang for providing cDNA of human Usp18, Dr. Barbara Frederick for providing SCC2 cells, and Melissa Adams for help in preparing the manuscript. J.E.D. is supported by National Cancer Institute/National Research Service Award F32CA126344, and A. S. is supported by National Cancer Institute grant CA-089151 and American Cancer Society grant RSG-00-247-04-CSM.

REFERENCES

Alwan, H. A., and van Leeuwen, J. E. (2007). UBPY-mediated epidermal growth factor receptor (EGFR) de-ubiquitination promotes EGFR degradation. J. Biol. Chem. *282*, 1658–1669.

Batra, S. K., Castelino-Prabhu, S., Wikstrand, C. J., Zhu, X., Humphrey, P. A., Friedman, H. S., and Bigner, D. D. (1995). Epidermal growth factor ligand-independent, unregulated, cell-transforming potential of a naturally occurring human mutant EGFRvIII gene. Cell Growth Differ. *6*, 1251–1259.

Beckham, C. J., and Parker, R. (2008). P bodies, stress granules, and viral life cycles. Cell Host Microbe *3*, 206–212.

Boese, Q., Samarsky, D., Huang, F., and Sorkin, A. (2006). siARRAY reverse transfection format (RTF): a rapid method for RNAi-based high-throughput studies of biological pathways. Nat. Methods Appl. Notes 2006 Vol. 1, an37–an38.

Bowers, K., Piper, S. C., Edeling, M. A., Gray, S. R., Owen, D. J., Lehner, P. J., and Luzio, J. P. (2006). Degradation of endocytosed epidermal growth factor and virally ubiquitinated major histocompatibility complex class I is independent of mammalian ESCRTII. J. Biol. Chem. *281*, 5094–5105.

Dikic, I., and Giordano, S. (2003). Negative receptor signalling. Curr. Opin. Cell Biol. *15*, 128–135.

Frederick, B. A., Helfrich, B. A., Coldren, C. D., Zheng, D., Chan, D., Bunn, P. A., Jr., and Raben, D. (2007). Epithelial to mesenchymal transition predicts gefitinib resistance in cell lines of head and neck squamous cell carcinoma and non-small cell lung carcinoma. Mol. Cancer Ther. *6*, 1683–1691.

Galperin, E., Verkhusha, V. V., and Sorkin, A. (2004). Three-chromophore FRET microscopy to analyze multiprotein interactions in living cells. Nat. Methods *1*, 209–217.

Grandis, J. R., and Sok, J. C. (2004). Signaling through the epidermal growth factor receptor during the development of malignancy. Pharmacol. Ther. *102*, 37–46.

Guo, J., Hui, D. J., Merrick, W. C., and Sen, G. C. (2000). A new pathway of translational regulation mediated by eukaryotic initiation factor 3. EMBO J. *19*, 6891–6899.

Huang, F., Jiang, X., and Sorkin, A. (2003). Tyrosine phosphorylation of the beta2 subunit of clathrin adaptor complex AP-2 reveals the role of a di-leucine motif in the epidermal growth factor receptor trafficking. J. Biol. Chem. *278*, 43411–43417.

Huang, F., Khvorova, A., Marshall, W., and Sorkin, A. (2004). Analysis of clathrin-mediated endocytosis of epidermal growth factor receptor by RNA interference. J. Biol. Chem. *279*, 16657–16661.

Huang, F., Kirkpatrick, D., Jiang, X., Gygi, S., and Sorkin, A. (2006). Differential regulation of EGF receptor internalization and degradation by multiubiquitination within the kinase domain. Mol. Cell *21*, 737–748.

Jakymiw, A., Lian, S., Eystathioy, T., Li, S., Satoh, M., Hamel, J. C., Fritzler, M. J., and Chan, E. K. (2005). Disruption of GW bodies impairs mammalian RNA interference. Nat. Cell Biol. *7*, 1267–1274.

Kedersha, N. L., Gupta, M., Li, W., Miller, I., and Anderson, P. (1999). RNA-binding proteins TIA-1 and TIAR link the phosphorylation of eIF-2 alpha to the assembly of mammalian stress granules. J. Cell Biol. *147*, 1431–1442.

Kefas, B. *et al*. (2008). microRNA-7 inhibits the epidermal growth factor receptor and the Akt pathway and is down-regulated in glioblastoma. Cancer Res. *68*, 3566–3572.

Knobeloch, K. P., Utermohlen, O., Kisser, A., Prinz, M., and Horak, I. (2005). Reexamination of the role of ubiquitin-like modifier ISG15 in the phenotype of UBP43-deficient mice. Mol. Cell. Biol. *25*, 11030–11034.

Komada, M. (2008). Controlling receptor downregulation by ubiquitination and deubiquitination. Curr. Drug. Discov. Technol. *5*, 78–84.

Liu, J., Rivas, F. V., Wohlschlegel, J., Yates, J. R., 3rd, Parker, R., and Hannon, G. J. (2005a). A role for the P-body component GW182 in microRNA function. Nat. Cell Biol. *7*, 1261–1266.

Liu, J., Valencia-Sanchez, M. A., Hannon, G. J., and Parker, R. (2005b). MicroRNA-dependent localization of targeted mRNAs to mammalian P-bodies. Nat. Cell Biol. *7*, 719–723.

Liu, L. Q., Ilaria, R., Jr., Kingsley, P. D., Iwama, A., van Etten, R. A., Palis, J., and Zhang, D. E. (1999). A novel ubiquitin-specific protease, UBP43, cloned from leukemia fusion protein AML1-ETO-expressing mice, functions in hematopoietic cell differentiation. Mol. Cell. Biol. *19*, 3029–3038.

Malakhov, M. P., Malakhova, O. A., Kim, K. I., Ritchie, K. J., and Zhang, D. E. (2002). UBP43 (USP18) specifically removes ISG15 from conjugated proteins. J. Biol. Chem. *277*, 9976–9981.

Malakhova, O. A., Kim, K. I., Luo, J. K., Zou, W., Kumar, K. G., Fuchs, S. Y., Shuai, K., and Zhang, D. E. (2006). UBP43 is a novel regulator of interferon signaling independent of its ISG15 isopeptidase activity. EMBO J. *25*, 2358–2367.

Malakhova, O. A., Yan, M., Malakhov, M. P., Yuan, Y., Ritchie, K. J., Kim, K. I., Peterson, L. F., Shuai, K., and Zhang, D. E. (2003). Protein ISGylation modulates the JAK-STAT signaling pathway. Genes Dev. *17*, 455–460.

McCullough, J., Clague, M. J., and Urbe, S. (2004). AMSH is an endosome-associated ubiquitin isopeptidase. J. Cell Biol. *166*, 487–492.

Mizuno, E., Iura, T., Mukai, A., Yoshimori, T., Kitamura, N., and Komada, M. (2005). Regulation of epidermal growth factor receptor down-regulation by UBPY-mediated deubiquitination at endosomes. Mol. Biol. Cell *16*, 5163–5174.

Nagane, M., Coufal, F., Lin, H., Bogler, O., Cavenee, W. K., and Huang, H. J. (1996). A common mutant epidermal growth factor receptor confers enhanced tumorigenicity on human glioblastoma cells by increasing proliferation and reducing apoptosis. Cancer Res. *56*, 5079–5086.

Nishikawa, R., Ji, X. D., Harmon, R. C., Lazar, C. S., Gill, G. N., Cavenee, W. K., and Huang, H. J. (1994). A mutant epidermal growth factor receptor common in human glioma confers enhanced tumorigenicity. Proc. Natl. Acad. Sci. USA *91*, 7727–7731.

Parker, R., and Sheth, U. (2007). P bodies and the control of mRNA translation and degradation. Mol. Cell *25*, 635–646.

Pelkmans, L., Fava, E., Grabner, H., Hannus, M., Habermann, B., Krausz, E., and Zerial, M. (2005). Genome-wide analysis of human kinases in clathrin- and caveolae/raft-mediated endocytosis. Nature *436*, 78–86.

Piecyk, M. *et al*. (2000). TIA-1 is a translational silencer that selectively regulates the expression of TNF-alpha. EMBO J. *19*, 4154–4163.

Pillai, R. S., Bhattacharyya, S. N., Artus, C. G., Zoller, T., Cougot, N., Basyuk, E., Bertrand, E., and Filipowicz, W. (2005). Inhibition of translational initiation by Let-7 MicroRNA in human cells. Science *309*, 1573–1576.

Ritchie, K. J., and Zhang, D. E. (2004). ISG *15*, the immunological kin of ubiquitin. Semin. Cell Dev. Biol. *15*, 237–246.

Row, P. E., Prior, I. A., McCullough, J., Clague, M. J., and Urbe, S. (2006). The ubiquitin isopeptidase UBPY regulates endosomal ubiquitin dynamics and is essential for receptor down-regulation. J. Biol. Chem. *281*, 12618–12624.

Rowinsky, E. K. (2004). The erbB family: targets for therapeutic development against cancer and therapeutic strategies using monoclonal antibodies and tyrosine kinase inhibitors. Annu. Rev. Med. *55*, 433–457.

Schwer, H., Liu, L. Q., Zhou, L., Little, M. T., Pan, Z., Hetherington, C. J., and Zhang, D. E. (2000). Cloning and characterization of a novel human ubiquitin-specific protease, a homologue of murine UBP43 (Usp18). Genomics *65*, 44–52 [correction published in Genomics (2007) *89*, 439].

Sorkin, A., and Von Zastrow, M. (2002). Signal transduction and endocytosis: close encounters of many kinds. Nat. Rev. Mol. Cell Biol. *3*, 600–614.

Sorkina, T., Miranda, M., Dionne, K. R., Hoover, B. R., Zahniser, N. R., and Sorkin, A. (2006). RNA interference screen reveals an essential role of Nedd4-2 in dopamine transporter ubiquitination and endocytosis. J. Neurosci. *26*, 8195–8205.

Stoscheck, C. M., and Carpenter, G. (1984a). Characterization of the metabolic turnover of epidermal growth factor receptor protein in A-431 cells. J. Cell. Physiol. *120*, 296–302.

Stoscheck, C. M., and Carpenter, G. (1984b). Down regulation of epidermal growth factor receptors: direct demonstration of receptor degradation in human fibroblasts. J. Cell Biol. *98*, 1048–1053.

Weiss, G. J. *et al*. (2008). EGFR regulation by microRNA in lung cancer: correlation with clinical response and survival to gefitinib and EGFR expression in cell lines. Ann. Oncol. *19*, 1053–1059.

Wiley, H. S. (2003). Trafficking of the ErbB receptors and its influence on signaling. Exp. Cell Res. *284*, 78–88.

Yamazaki, H., Ohba, Y., Tamaoki, N., and Shibuya, M. (1990). A deletion mutation within the ligand binding domain is responsible for activation of epidermal growth factor receptor gene in human brain tumors. Jpn. J. Cancer Res. *81*, 773–779.

Zhao, C., Denison, C., Huibregtse, J. M., Gygi, S., and Krug, R. M. (2005). Human ISG15 conjugation targets both IFN-induced and constitutively expressed proteins functioning in diverse cellular pathways. Proc. Natl. Acad. Sci. USA *102*, 10200–10205.